

Hydrogen chemisorption on Si(111)-(7×7) and -(1×1) surfaces. A comparative infrared study

Y. J. Chabal, G. S. Higashi, and S. B. Christman

Bell Laboratories, Murray Hill, New Jersey 07974

(Received 11 July 1983)

A comparative study of hydrogen vibrations on the Si(111)-(7×7) and the laser-annealed Si(111)-(1×1) surfaces has been carried out by means of high-resolution infrared spectroscopy. The two surfaces have similar initial sticking coefficients and for the most part are characterized by broad distributions of chemisorption sites. However, clear differences between the two surfaces are observed. Two distinct adsorption sites can be isolated on the 7×7 surface while only one well-defined site is present on the laser-annealed surface. Diffusion of a small amount of hydrogen below the outermost silicon layer appears to take place on the 7×7 surface but is not observed on the laser-annealed surface. From this study new insights about the 7×7 reconstruction are obtained.

I. INTRODUCTION

The surface geometry of the Si(111), whether thermally annealed 7×7 or laser-annealed 1×1, is not well understood.¹ In particular, the question of whether the 1×1 surface is essentially unreconstructed as first proposed by Zehner *et al.*² or reconstructed with no long-range order³⁻⁶ has been a subject of controversy. From low-energy electron-diffraction (LEED) *I-V* measurements Zehner *et al.*² concluded that the outermost layer was a perfect termination of the bulk with a 25% contraction. In contrast, angle-integrated photoemission data showed that the electronic structure below the top of the valence band is very similar for both surfaces.³ Medium-energy ion scattering combined with channeling and blocking also showed that the local reconstruction is indeed very similar on both surfaces.⁴ Thus despite the LEED interpretation, there is strong experimental evidence for local reconstruction on the 1×1 surface similar to that on the 7×7 surface. However, there is a shoulder near E_F in the surface electronic structure of the 7×7 surface which is totally absent on the 1×1 surface.^{5,6} Additionally, although the general profile of the ion scattering is similar for both surfaces, the number of atoms per row displaced from the bulk positions appear slightly higher for the 7×7 surface. Therefore, although the local structure appears to be very similar on both surfaces, there are small but definite differences which are not understood.

A sensitive way to compare two similar surfaces is to monitor the properties of chemisorbed species. By choosing a small atom which perturbs the surface minimally, such as hydrogen, one may expect to learn about the local reconstruction of the clean surfaces and their behavior as a function of coverage. For example, electron-energy-loss spectroscopy (EELS) has shown that dihydride is formed on the Si(111)-(7×7) surface at moderate coverages,⁷ indicating the presence of two dangling bonds on the associated surface silicon atoms. Recently, high-resolution infrared spectroscopy has indicated that the initial adsorp-

tion involves the formation of monohydride in a unique chemisorption site within the 7×7 unit cell.⁸ Because of the high resolution of this technique differences between chemisorption sites can easily be distinguished. Thus, by performing comparative infrared studies of hydrogen chemisorption on the 1×1 and 7×7 surfaces, one may expect to bring out subtle differences in local chemical bonding.

We present here a study of hydrogen chemisorption on the Si(111)-(7×7) and -(1×1) surfaces by infrared spectroscopy. We find that, in accord with the photoemission and ion-scattering results, the two surfaces display many similarities but also show substantial differences. At saturation coverage, for example, most of the chemisorbed hydrogen resides in an inhomogeneous distribution of sites on both surfaces. However, the 7×7 surface appears to be more "porous" than the 1×1 surface, allowing the incorporation of subsurface hydrogen. At lower coverages hydrogen chemisorbs at *well-defined* sites on both surfaces. Yet, while two sites can clearly be identified on the 7×7 surface, only a single site is observed on the 1×1 surface. Comparison of the results on the 7×7 and 1×1 surfaces suggests that clear differences in the *local geometry* exist and extend beyond the outermost layer.

II. EXPERIMENTAL

The experimental apparatus is comprised of a modified Nicolet 6000 interferometer with an ultimate resolution of 0.1 cm^{-1} and an ultrahigh vacuum (UHV) chamber.⁸⁻¹⁰ The nitrogen-purged interferometer covers the region 200–15 000 cm^{-1} with two different beam splitters (Ge on CsI and Si on quartz) using a standard globar infrared source. The collimated infrared radiation exiting the interferometer is focussed through the entrance CsI window of the UHV chamber onto the sample and recollimated through another CsI window before being detected by the infrared detector. Three detectors are used to cover the broad spectral range of the interferometer—Ge:Cu from

200 to 1000 cm^{-1} , HgCdTe from 700 to 5000 cm^{-1} , and InSb from 2000 to 15000 cm^{-1} . For the experiments presented in this paper only the Ge-on-CsI beam splitter was used in conjunction with the HgCdTe detector. The two infrared windows are sealed with a differentially pumped O-ring arrangement.¹¹ The system is equipped with two 400-l/sec ion pumps and a Ti sublimator with a cold shroud for pumping in addition to a rearview LEED spectrometer as well as Auger and mass spectrometers for sample and ambient characterization. The sample manipulator holds the sample 2 in. off axis with the capability of resistive heating to 1400°C and cooling to 20 K.¹⁰

The sample geometry is shown in Fig. 1. *p*-type silicon wafers ($\rho = 1700 \Omega \text{ cm}$) are cut in a U shape (3.8 cm long by 1.5 cm wide) so that uniform resistive heating of the area under study can be achieved (better than 10° stability over 90% of the surface). The ends are polished at 40° with respect to the surface normal so as to allow the infrared radiation to penetrate into the sample, internally reflect off both the front and back surfaces, and exit on the other side. The sample thickness is 0.5 mm. The infrared radiation is externally incident at a 30° angle resulting in a 37° internal incidence angle and 50 bounces on the front surface alone. This internal angle gives roughly equal weight to the various components of the field for both *s* and *p* polarizations.¹² As shown on the bottom of Fig. 1, *p*-polarized radiation can probe modes both parallel and perpendicular to the surface while *s*-polarized radiation is only sensitive to modes parallel to the surface. However, the study of modes below 1000 cm^{-1} is not possible with this geometry for silicon because of a weak lattice absorption.¹³ This absorption is only restrictive for very long path lengths within bulk silicon and can be used advantageously to align the sample within the UHV system.

The front surface of the sample was cleaned by mild grazing incidence argon-ion sputtering (10 $\mu\text{A}/\text{cm}^2$, 0.5 kV for 3 min) with the sample held at room temperature to remove the native oxide followed by an extended an-

nealing at 800°C (~1 h). Note that in order to sputter its full area, the sample had to be translated during sputtering. The sputtering and annealing treatment preserve the back-surface native oxide (~15 Å thick). Auger analysis was performed with a single-pass cylindrical mirror analyzer with an ultimate sensitivity of about 0.1% monolayer (ML) for the common impurities. After the regular surface preparation, about 0.3% ML of carbon remained over the full area of the sample. This level could be reduced by laser annealing, but no differences in the subsequent infrared spectra were detected, indicating that these levels of carbon do not affect surface properties in an observable way. Atomic hydrogen exposures were performed by valving off the ion pumps and filling the chamber with 2×10^{-7} Torr molecular hydrogen H_2 while heating (to 2000 K) a tungsten ribbon ($1 \times 2 \text{ cm}^2$) placed 4 cm in front of the sample. Contaminants, mostly CO and H_2O , remained at less than 1×10^{-10} Torr partial pressure during exposures due to the high pumping speed of the cooled-titanium sublimation pump. The molecular hydrogen was then quickly pumped out by means of a turbomolecular pump and a base pressure of less than 1×10^{-10} Torr was reached within a few minutes.

All the infrared spectra were taken in a differential mode where a reference spectrum $I_0(\nu)$ of the clean surface was taken first, then after a specified exposure the spectrum associated with the hydrogen-covered surface $I(\nu)$ was recorded. The symbol ν represents the infrared radiation frequency. Finally, the surface was flashed at 800°C and another reference spectrum $I_0(\nu)$ was taken. The normalized induced spectrum is then

$$\frac{\Delta R'}{R'}(\nu) = \frac{I(\nu) - I_0(\nu)}{I_0(\nu)}$$

However, as described elsewhere,¹⁴ the reference spectra may contain electronic absorption due to the surface states which are quenched on the hydrogen-covered surface. This change in absorption, then, also appears in the hydrogen-induced spectrum, $\Delta R'(\nu)/R'(\nu)$. This contribution can be isolated by measuring the normalized spectrum of oxygen-covered Si(111) where no vibrational lines associated with the oxygen are present in the frequency range under study (1500–3000 cm^{-1}). The oxygen-covered surface reveals that this electronically induced absorption is, in fact, very broad (greater than 1000 cm^{-1}) without any sharp structure and can be approximated in the region of the silicon hydrogen vibrations as a straight-line background. The vibrational contribution to the hydrogen-induced spectrum is thus given to a very good approximation in a small frequency range ν_1 to ν_2 by

$$\frac{\Delta R}{R}(\nu) = \frac{I(\nu) - I'_0(\nu)}{I'_0(\nu)}$$

with

$$I'_0(\nu) = I(\nu_1) + (\nu - \nu_1) \frac{I(\nu_2) - I(\nu_1)}{\nu_2 - \nu_1}$$

The infrared transmission spectrum $I(\nu)$ often contains interference fringes (channeled spectra) due to the various optical elements in the beam with a typical amplitude 1%

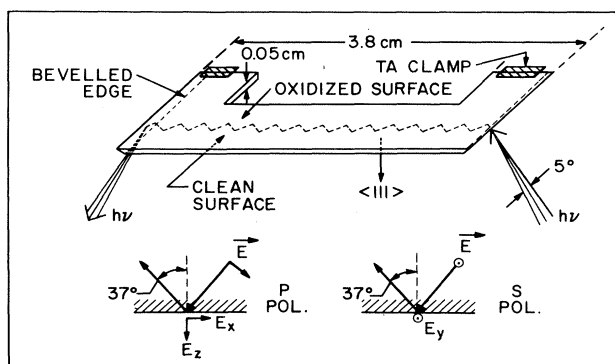


FIG. 1. Schematic representation of the sample geometry. Radiation is incident on the input beveled edge and bounces 50 times on the surface under study with an internal angle of incidence $\theta = 37^\circ$ before exiting through the output beveled edge. Back surface is kept oxidized. Electromagnetic field distributions are shown at the bottom for the two polarizations used.

of the total intensity. Small temperature variation and/or small motions of the sample from run to run will affect the optical path enough that imperfect ratioing of these fringes occurs, resulting in oscillations in the data. These regularly spaced oscillations observed in some of the spectra presented in the next section are not intrinsic to the chemisorbed hydrogen spectra and should be ignored. In bad cases when the oscillations are large compared to the features under consideration, the characteristic signature in the interferogram is removed and replaced by a straight line over a narrow region. In this manner the fringes are eliminated both in hydrogen-induced and reference spectra so that the normalized induced spectrum is free from oscillations with only a minimal loss of information about the sharp hydrogen vibrational features.¹⁵

Calibration of the coverage was done in two independent ways. First, the LEED patterns obtained for various exposures were compared to the calibrated patterns of Culbertson *et al.*,¹⁶ who used nuclear microanalysis for absolute coverage measurement. From 0.4 ML to saturation coverage (1.25 ML), the comparison could be made with 10% accuracy. Below 0.4 ML extrapolation assuming a simple Langmuir dependence yielded 15% accuracy. Second, the total integrated infrared absorption of the Si-H stretch mode associated with saturation coverage was measured, properly taking into account the field strengths parallel and perpendicular to the surface. *Under the assumption that the dynamic dipole moment of the SiH mode does not change with coverage*, the coverage can thus be determined with 10% accuracy for lower exposures. The assumption that the dynamic dipole moment does not vary significantly from low to high coverage can be tested by measuring the infrared absorption on the hydrogen-saturated Si(100) surface which is known to form a dihydride.^{9,17} By comparing the normalized infrared absorption for these two very different surfaces, an upper limit on the possible variation of the dynamic dipole moment with surface silicon atom rearrangement can be established. Again, the absolute coverage on the Si(100) surface is accurately known from nuclear microanalysis.¹⁸ The absorption strength per SiH unit was found to be within 15% of that found on the hydrogen-covered Si(111) surface. Therefore, an upper limit of $\pm 20\%$ error can be assigned to the absolute coverage obtained using the integrated absorption of the vibrational mode. The agreement of the two methods (LEED microanalysis and ir absorption) is well within the error bars.

Laser-annealing experiments were performed with a frequency-doubled (532-nm) neodymium:yttrium-aluminum-garnet (Nd:YAG) laser, which provided (7–8)-nsec pulses at a repetition rate of 10 Hz. The output of the laser was passed through a polarizing-prism optical attenuator and was subsequently apertured to illuminate the sample with a crescent-shaped segment of the laser's "doughnut" mode. The vertical crescent was approximately 4 mm tall and 0.5 mm wide with a fluence which could easily be adjusted in the range between 100 and 600 mJ/cm². The 7 \times 7-to-1 \times 1 transition was found to occur at a fluence at the sample of ~ 350 mJ/cm², in reasonable agreement with previously published results.^{19,5} The preparation of the 1 \times 1 sample surface was performed at

440 mJ/cm², exposing the entire surface to be probed by the infrared by translating the laser beam across the sample at a fixed rate of ~ 0.5 mm/sec. At this rate of translation the sample experiences approximately ten laser shots on any given area. No visible sample damage was observed at this fluence even after as many as five passes of the laser.

III. EXPERIMENTAL RESULTS

Our findings can be divided into two distinct classes according to whether or not the clean 7 \times 7 or 1 \times 1 surfaces experience substantial alteration with hydrogen coverage. For very low coverages ($\Theta < 0.15$), the 7 \times 7 LEED pattern shows no noticeable changes in the relative intensity of the seventh-order spots, indicating that the silicon surface atoms have not moved appreciably.⁸ At higher coverages or upon light thermal annealing (200–350°C) subsequent to hydrogen exposure, the LEED patterns show definite differences from the patterns of clean 7 \times 7 surfaces. Similarly in the case of the 1 \times 1 surface, the weak background centered at half-order disappears for high exposures. Since the electrons are not scattered by hydrogen, the alterations in the LEED patterns must arise from hydrogen-induced changes in the position of surface silicon atoms within the unit cell. We shall, therefore, separate the low-coverage data with no LEED-pattern changes and the data taken at high coverages with and without subsequent annealing where the LEED patterns are substantially altered.

Typical data taken using *p* polarization in the low-coverage regime are shown in Fig. 2 where the absorptions induced by 5% of a ML of hydrogen on the 7 \times 7 and 1 \times 1 surfaces are plotted. Two lines are observed on the 7 \times 7 surface—one at 2073 cm⁻¹ and the other at 2077 cm⁻¹. In contrast, only a single symmetric line at 2077

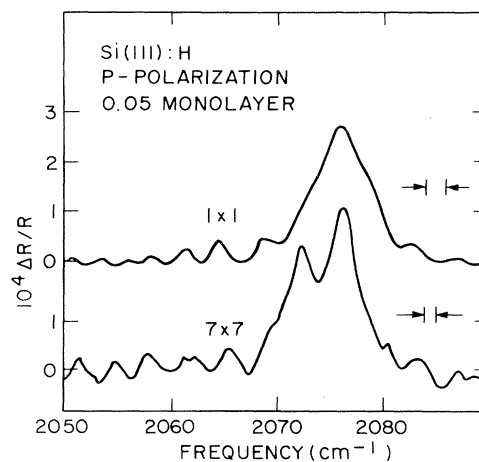


FIG. 2. Reflectivity change for 5% ML on the laser-annealed 1 \times 1 and the thermally annealed 7 \times 7 surfaces. Note the change of resolution. There is no corresponding absorption on either surface when *s*-polarized radiation is used.

cm^{-1} appears on the 1×1 surface. Although all linewidths are of similar magnitude, the single line on the 1×1 surface is $\sim 50\%$ broader than those on the 7×7 surface. The linewidths on either of these surfaces show no temperature dependence in the range 77–300 K, characteristic of inhomogeneous broadening. Under identical exposure conditions the integrated absorption strength on the 1×1 surface is equal to that on the 7×7 , indicating very similar hydrogen-sticking coefficients. Of greater interest is the fact that absolutely no hydrogen-induced absorption is observed using *s*-polarized light in this coverage regime ($\Theta < 0.15$ ML). Thus on both the 7×7 and the 1×1 surfaces the silicon-hydrogen modes are polarized purely perpendicular to the surface.

At saturation coverages the 7×7 surface exhibits seventh-order spots only in the immediate vicinity of the integral-order spots,²⁰ while the laser-annealed surface is characterized by a *very weak* and uniform background with a disappearance of the half-order feature.⁵ Corresponding to these changes in the LEED patterns, dramatically different infrared spectra are observed. For saturation coverage, for instance, one observes a broad background centered at about 2100 cm^{-1} on both the 7×7 and 1×1 surfaces (Fig. 3). At lower frequencies the two surfaces also differ. Whereas a well-defined band centered at 1970 cm^{-1} appears at saturation on the 7×7 surface, no such band is present on the 1×1 surface (Fig. 3). This extra contribution was consistently observed on the 7×7 surface, independent of the preparation conditions. In contrast, only a small *flat* background appears on the 1×1 surface even after extremely large exposures. The other clear difference between the 7×7 and 1×1 surfaces is seen in the sharp structure at 2082 cm^{-1} on the 1×1 surface, which occurs as a much broader peak centered at 2085 cm^{-1} on the 7×7 surface.

These features are studied in greater detail in Figs. 4 and 5 for the 1×1 and 7×7 surfaces, respectively. Let us first focus our attention on the curves labeled *c* in Fig. 4 where the absorptions induced by a saturation coverage on

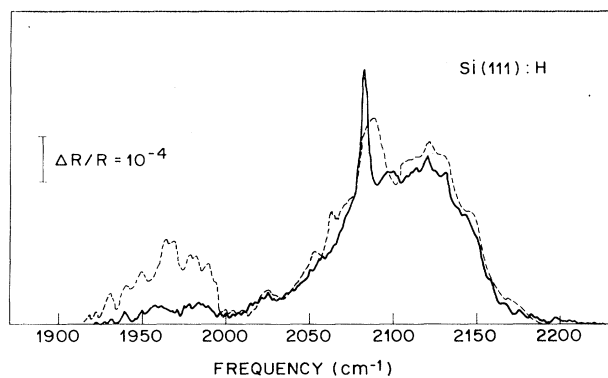


FIG. 3. Reflectivity change induced by a saturation coverage of hydrogen on the two Si(111) surfaces. Solid line is for the laser-annealed 1×1 surface with a coverage of 1.0 ML. Dashed line is for the thermally annealed 7×7 surface with a coverage of 1.25 ML (see text). Radiation is *p*-polarized.

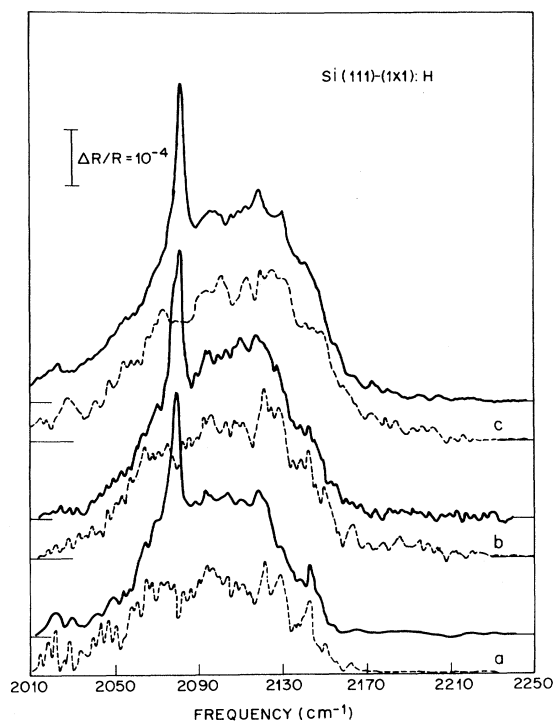


FIG. 4. Reflectivity change induced by hydrogen chemisorption on the laser annealed 1×1 surface for curves *a*, $\Theta = 0.6$ ML, *b*, $\Theta = 0.8$ ML, and *c*, $\Theta = 1.0$ ML. Components parallel to the surface (*s*-polarization) are shown in dashed lines and displaced downward for clarity.

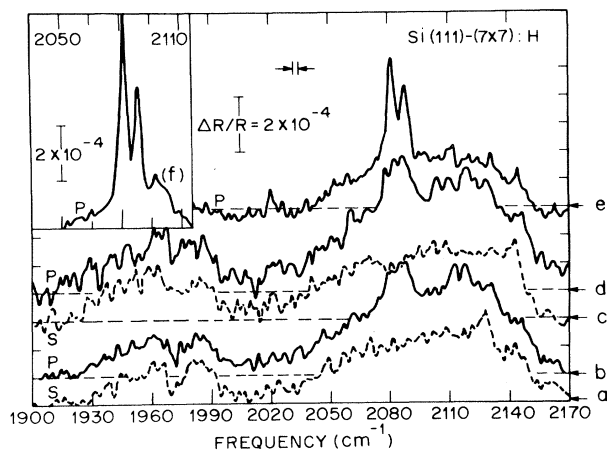


FIG. 5. Reflectivity change induced by hydrogen chemisorption on the 7×7 surface. Curve *a*—*s*-polarized data for $\Theta = 1.1$ ML; curve *b*—*p*-polarized data for $\Theta = 1.1$ ML; curve *c*—*s*-polarized data for $\Theta = 1.25$ ML; curve *d*—*p*-polarized data for $\Theta = 1.25$ ML; curve *e*—*p*-polarized data for $\Theta = 1.25$ ML plus anneal to 200°C ; and curve *f*—*p*-polarized data for further anneal to 350°C .

the 1×1 surface are plotted for both s and p polarization. The absence of the sharp peak at 2082 cm^{-1} in the s -polarized data clearly indicates that this vibration occurs perpendicular to the surface. A similar behavior is observed for the peak at 2085 cm^{-1} on the 7×7 surface, as can be seen by comparing curves c and d of Fig. 5. Further, the integrated area under these sharp modes perpendicular to the surface is equal for each surface to that measured on its counterpart for $\Theta \sim 0.15 \text{ ML}$. This absorption strength was previously established to correspond to four to five atoms per unit cell in the case of the 7×7 surface⁸ and corresponds to 9% ML both on the 7×7 and 1×1 surfaces. The broader line centered at 2085 cm^{-1} on the 7×7 surface (curve d in Fig. 5) is actually made up of two lines—one at 2082 cm^{-1} and the other at 2088 cm^{-1} , as can be seen if one lightly anneals these hydrogen covered surfaces (curve e and inset curve f of Fig. 5). The annealing process tends to diminish the broad background, as it sharpens up these peaks. In fact, in curve f in the inset of Fig. 5 the remaining coverage is only a quarter of a monolayer, as opposed to the initial 1.25 ML, and all the absorption is polarized perpendicular to the surface. The low-frequency band at around 1970 cm^{-1} is no longer present on the lightly annealed 7×7 surfaces. Note that all of the broad-background-like features exhibit strong polarizations parallel to the surface.

To try to understand the origin of the sharp features on top of the broad background at saturation coverages annealing experiments were performed on low-coverage surfaces where the background is negligible. The question is why on the 7×7 surface, for example, the peaks occur at 2073 and 2077 cm^{-1} at low coverage whereas they occur at 2082 and 2088 cm^{-1} at high coverage? The results for $\Theta = 0.15$ are presented in Fig. 6 where the solid curves show the hydrogen-induced absorption before annealing, and the dashed curves show the absorption after annealing. Before annealing this coverage corresponds to the maximum observed peak height at 2077 cm^{-1} and occurs prior to the weakening of the $\frac{3}{7}$ and $\frac{4}{7}$ LEED spots. The 2077-cm^{-1} line of the 7×7 surface is observed to exhibit a shoulder at $\sim 2073 \text{ cm}^{-1}$. The area under this feature (line plus shoulder) corresponds to 4.5 atoms per 7×7 unit cell, as compared with the seven atoms per unit cell one would obtain integrating all the absorption observed. Similar observations can be made on the laser-annealed surface with the exception that no shoulder is found on the line at 2077 cm^{-1} . After annealing at 350°C for 1 min, the 7×7 surface rearranges itself to give two lines, one at 2080 cm^{-1} and the other at 2086 cm^{-1} . This behavior is reminiscent of that of the annealed high-coverage 7×7 surface. A similar annealing treatment of the 1×1 surface again reveals only a single peak, but now near 2080 cm^{-1} . In both cases annealing causes a substantial shift towards higher frequencies although the resulting lines are still $1\text{--}2 \text{ cm}^{-1}$ lower than that obtained at saturation coverage. Finally, it should be noted that there is a slight loss in absorption strength after the annealing process. This is probably due to hydrogen desorption from the central regions of the sample which get slightly hotter than the outer edges.

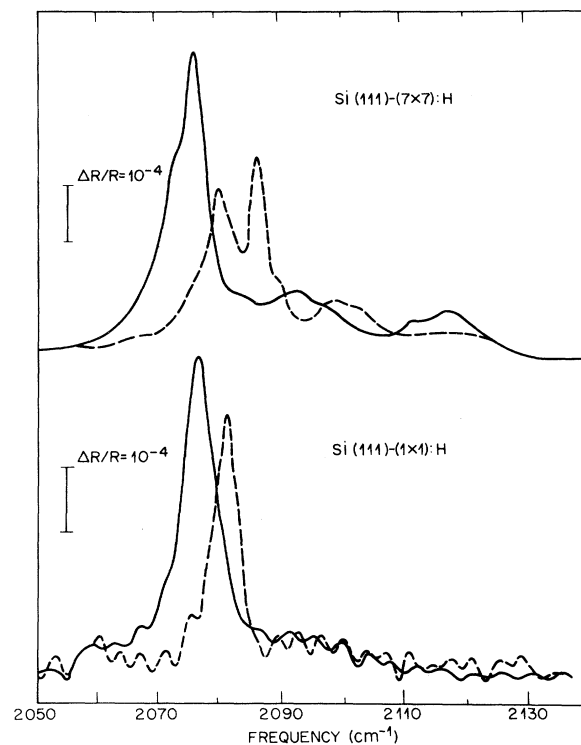


FIG. 6. Reflectivity change induced by 0.15 ML of hydrogen on the 7×7 and 1×1 surfaces upon room-temperature adsorption (solid lines) and subsequent annealing to 350°C for 1 min (dashed lines). Spectra are taken with the sample at room temperature and p -polarized radiation.

IV. DISCUSSION

For low enough coverages ($\Theta < 0.15 \text{ ML}$) the clean Si(111) surfaces are not substantially altered by the presence of the hydrogen, and thus by studying the Si-H vibrations direct information on the presence and polarization of *clean-surface* dangling bonds can be obtained.⁸ In contrast, spectra induced by higher coverages and/or annealing will illustrate the cooperative effects of the *silicon-hydride surface* in which silicon surface atoms rearrange themselves to assume configurations of lower energy.

A. Low-coverage regime

Focusing first on the 7×7 surface, the low-coverage spectra are characterized by two absorption lines polarized perpendicular to the surface. The lower-frequency line at 2073 cm^{-1} , which saturates at one atom per unit cell, has been attributed to a dangling bond recessed below the outermost layer.⁸ This line is totally absent on the laser-annealed surface at any coverage, whereas a well-defined line at 2077 cm^{-1} is observed on both the 7×7 and 1×1 surfaces (Fig. 2). We have postulated that the 2073-cm^{-1} line has its origin connected with the long-range nature of the 7×7 reconstruction and is probably located at the corner of the 7×7 unit cell⁸; in contrast, the line at 2077

cm^{-1} would be associated with a well-defined *local* structure. Indeed, while ion-scattering experiments⁴ show that the two surfaces are *locally* similar, LEED data emphasize that the *long-range* order is different.

Thus, from the infrared data concerning the 2077-cm^{-1} mode, it can be inferred that the 7×7 unit cell is made up of small identical subunits with a well-defined chemisorption site polarized perpendicular to the surface. By integrating the area under the 2077-cm^{-1} line at saturation ($\Theta=0.15$ ML), not including the broad background, it can be concluded that three to four such subunits are present on the 7×7 unit cell. On the laser-annealed surface these subunits are also well formed resulting in another line at 2077 cm^{-1} . The local disorder is slightly increased as reflected in a 50% broader line, but is still very much typical of inhomogeneities occurring upon room-temperature atomic hydrogen exposures. For example, the measured linewidth on this 1×1 surface, $\Delta=6\text{ cm}^{-1}$, is very close to that measured on the Si(100) surface ($\Delta=5\text{ cm}^{-1}$) after exposure to atomic hydrogen.⁹ The idea that the 7×7 unit cell is comprised of smaller subunits which are present on the laser-annealed surface is supported by the fact that if we consider a unit area on the surface containing 49 surface atoms, integration of the 2077-cm^{-1} line shows that four to five subunits are present, i.e., one more subunit per 49 atoms than on the 7×7 unit cell. This extra subunit may occur in place of the site associated with the 2073-cm^{-1} mode developed on the 7×7 unit cell so that on the average there is one more subunit per 49 surface atoms on the laser-annealed surface.

The data presented so far does not preclude a situation where the hydrogens contributing to the 2077-cm^{-1} line all belong to the same short-range structure, i.e., to only a single structure which would then be larger than the *separate* subunits proposed. To distinguish between separate small subunits and a larger structure encompassing three to four well-defined sites the experiment could be repeated for widely different regrowth velocities (i.e., different laser powers) in which case the extent of the long-range order could be varied.²¹ This experiment was attempted with a 50% variation in regrowth velocity. In this range no changes in the infrared spectrum were observed upon chemisorption. However, by working close to the melting threshold, i.e., at a regrowth velocity of about 6 m/sec, we are led to believe that the surface order cannot be long ranged. This would tend to support an arrangement whereby the subunits responsible for the 2077-cm^{-1} line are small and distinct. Such subunits would then constitute the building blocks of the 7×7 reconstruction and the dominant *ordered* structure on the 1×1 surface. As a motivation for future work, the possibility that these subunits are responsible for the weak structured background at the half-order position in the LEED patterns of the laser-annealed surface could be considered. On the 7×7 the more intense $\frac{3}{7}$ and $\frac{4}{7}$ spots could in turn have the same origin.

The above observations regarding the 7×7 reconstruction would be in support of models which do show subunits within the 7×7 unit cell such as the milk-stool model,²² the vacancy model,²³ the terrace model,^{20,24} or some more recent proposals,²⁵⁻²⁷ except for the fact that

the number of subunits is generally greater than three to four per unit cell. However, comparison with various models requires a more detailed understanding of the *chemical* activity of the dangling bonds arising from the reconstruction. With regard to the chemical activity of the reconstructed Si(111) surfaces themselves, we note that preferential adsorption is taking place in the low-coverage regime on sites polarized purely perpendicular to the surface, i.e., those forming only a monohydride. For $\Theta \leq 0.15$ ML, both the sharp features and the nascent broad background have *no* components parallel to the surface. In addition, the relative population of the sites characterized by the sharp lines is larger than that of the rest of the sites characterized by a broad background by a bigger factor than statistical expectations. For instance, for $\Theta=0.15$ ML, 60% of the hydrogen (4.5 atoms/unit cell) is adsorbed on these well-defined sites. The ratio is even higher at lower coverages. This indicates that there must be some surface diffusion taking place at room temperature allowing the hydrogen to bind to these special sites. To check this conjecture, exposures at 80 and 500 K were performed with corresponding large broad background for the low-temperature exposure and no background at all for the high-temperature exposure.

B. High-coverage data

The dominant features of the high-coverage data on both the 7×7 and 1×1 surfaces is the presence of a broad background centered around 2100 cm^{-1} exhibiting an absorption component parallel to the surface, the relative importance of which increases up to saturation (Figs. 3-5). The broad featureless background indicates that the hydrogen is chemisorbed in an inhomogeneous distribution of sites. Such a broadening may be due in part to surface etching as was observed on the Si(100) surface for very large exposures.⁹ However, the appearance of this broad background at coverages as low as 10-20% ML points to the fact that the 7×7 and 1×1 surfaces are intrinsically "rough," with a variety of chemisorption sites not present on the Si(100) surface, for instance. In particular, the presence of this broad background on the laser-annealed surface shows conclusively that the clean surface is not unreconstructed.² If surface atoms were in bulklike positions, only one infrared line polarized purely perpendicular to the surface with an integrated strength corresponding to one hydrogen per surface silicon atom should be observed. Instead, the broad band centered at 2100 cm^{-1} on the laser-annealed surface is similar to that observed on the 7×7 surface under similar exposure conditions. The origin of this broad background can be inferred in part from the infrared work⁹ on the Si(100) surface where the dihydride mode SiH_2 is observed with components perpendicular and parallel to the surface around 2100 cm^{-1} , and from the EELS work on the Si(111)-(7×7) surface where the scissor mode characteristic of the SiH_2 unit is observed.⁷ Part of the background can therefore be attributed to the presence of SiH_2 on a distribution of sites. The presence of steps with dangling bonds at some angle from the normal^{20,24} or the formation of trihydride²⁸ could also account for part of the observed back-

ground. Whatever the origin of this absorption at 2100 cm^{-1} , the infrared data shows that both the 7×7 and 1×1 surfaces behave similarly in this region.

This is not so for the other broad band centered at 1970 cm^{-1} which appears on the 7×7 surface only. This band can be assigned to vibrations of SiH *inside* the bulk based on the following facts. Firstly, as recently proposed,²⁹ the dielectric screening of the SiH mode will shift the stretching mode down by 100 cm^{-1} assuming a 3-\AA -diam. enclosure for the SiH unit. Secondly, recent observations of hydrogen chemisorbed on grain boundaries in *polycrystalline* silicon³⁰ showed an absorption band at 219 cm^{-1} which is substantially downshifted in frequency from the free-SiH mode occurring around 2100 cm^{-1} . Thirdly, a band centered at 1985 cm^{-1} in hydrogen-implanted *a*-Si is consistently observed over a wide range of hydrogen concentrations³¹ and has been assigned to the stretch mode of monohydride (SiH).³² The 1970-cm^{-1} band is consistent with hydrogen diffused below the outermost layer and forming SiH-type bonds. Stretching modes associated with SiH_2 and SiH_3 are located on the high-frequency side of the SiH stretch³³ and therefore cannot account for this low-frequency band.³⁴ The implications of this low-frequency band are important: The 7×7 unit cell would then be an open structure which makes the diffusion of hydrogen into subsurface layers possible. The laser-annealed surface is "smoother" in that diffusion below the top layer does not readily take place. One may speculate that the diffusion originates from the corner site of the 7×7 unit cell which is recessed below the surface.⁸ In any case, the integrated area associated with the 1970-cm^{-1} band accounts for most of the coverage above 1 ML observed with nuclear microanalysis,¹⁶ which cannot distinguish between chemisorbed hydrogen and hydrogen diffused below the top layer. It can thus be concluded that the average number of chemisorbed hydrogen *on top* of the 7×7 unit cell is one per silicon atom. This indicates that either the number of dangling bonds per unit cell is about 49 or else that hydrogen does not chemisorb on every available dangling bond. The latter is not inconceivable since this is precisely what was observed on the Si(100) surface¹⁸ where at most $\frac{3}{4}$ of the available dangling bonds can be occupied.

The other distinctive features of the high-coverage data are the sharp lines located at 2082 cm^{-1} for the laser-annealed surface and at 2085 cm^{-1} for the 7×7 surface (Fig. 3). These lines are distinct from the background both in sharpness and *polarization*. Since the integrated area under the 2082-cm^{-1} line (not including the background) is equal to that of the 2077-cm^{-1} line measured at $\Theta=0.15\text{ ML}$ on the laser-annealed surface, it is likely that the same SiH units are responsible for these lines both at low and high coverages. The shift of 5 cm^{-1} would then be due to atomic rearrangement of the surface silicon atoms. The sign and magnitude of the shift are typical of thermal-contraction-induced shifts. On the Si(100):H surface, for example, the symmetric stretch shifts from 2099 to 2102 cm^{-1} in going from 300 and 80 K,³⁵ i.e., for a lattice linear contraction of 2.3×10^{-4} . Thus, an atomic relaxation of the order of 10^{-3} \AA could account for such a shift. A modification of the surface electronic structure

at saturation coverage could also be responsible for such a shift. Although the microscopic origin of the shift is not understood, the 7×7 surface develops a second class of sites yielding the 2088-cm^{-1} line which does not exist on the laser-annealed surface. This second class of site is not a metastable structure since both the 2082- and 2088- cm^{-1} lines persist upon mild annealing to 350°C during which the silicon atoms can diffuse.³⁶ If the 7×7 and 1×1 surfaces differed only in the arrangement of the outermost layer, then one would expect that with hydrogen stabilization the configuration obtained after mild annealing would be similar. The fact that this 2088-cm^{-1} peak remains after annealing on the 7×7 surface indicates that the two surfaces have differences extending beyond the outermost layer. This observation is consistent with models of the 7×7 surface requiring the modification of several layers such as the model proposed by Bennett *et al.*,³⁷ which describes the 7×7 reconstruction as due to a four-layer wurzitelike stacking. Such a wurzite structure may not have the time to form to the same extent during the process of laser quenching with a typical quenching time of 50 psec per layer.²¹ Invoking differences over several layers for the two surfaces was also necessary to account for the band at 1970 cm^{-1} . From the infrared data it appears that the laser-annealed surface tends to form a near-surface structure which is more homogeneous than the 7×7 surface. The latter is a more open structure possibly stabilized by stacking faults³⁸ through which the hydrogen can diffuse more readily. The near-surface regrowth upon laser annealing, being more bulklike than that of the 7×7 surface, would account for the good fit of the *I-V* LEED data of Zehner *et al.*² to a bulklike structure. However, this suggestion is not born out by the ion-scattering data.⁴

We now address the question of whether the atoms contributing to the sharp lines polarized perpendicular to the surface observed at high coverage (2082 cm^{-1} for the 1×1 surface and $2082\text{--}2088\text{ cm}^{-1}$ for the 7×7 surface) are the same atoms responsible for the lines observed at low coverage (2077 cm^{-1} for the 1×1 surface and $2073\text{--}2077\text{ cm}^{-1}$ for the 7×7 surface). As noted earlier, the integrated area of these lines alone are equal at all coverages $\Theta \geq 0.15\text{ ML}$, i.e., after saturation. Further, Fig. 6 shows that annealing to 350°C will cause the lines to shift up in frequency to a position about 2 cm^{-1} below the saturation-coverage position, e.g., 2080 instead of 2082 cm^{-1} for the 1×1 surface. This implies that whether or not the SiH vibrators characterized by the sharp lines are the same at low and high coverages, the sharp lines do represent the *lowest-energy surface configuration* at high coverage. The 2-cm^{-1} difference between the annealed low-coverage data and high-coverage data is well accounted for by the dipole-dipole interactions present at saturation coverage⁹ consistent with the picture that the sharp lines arise from distinct subunits rather than a cluster of four or five atoms together.

V. CONCLUSIONS

This comparative vibrational study of hydrogen chemisorbed on the 7×7 and 1×1 surfaces shows that both

surfaces have strong similarities: The same initial sticking coefficient and a broad distribution of sites upon saturation which can be clearly distinguished from the much less inhomogeneous site distribution on the Si(100) surface at similar coverages. Both surfaces also form a monohydride at very low coverages. However, clear differences are found especially with regards to the small number of well-defined sites characterized by sharp absorption lines. Two distinct sites are present on the 7×7 surface while only one can be identified on the 1×1 surface, both at low and high coverages. The sites in common are believed to arise from small subunits each containing a well-defined chemisorption site, while the extra site present on the 7×7 surface is thought to result from a longer-range reconstruction.

The 7×7 reconstruction appears to have an open structure involving several layers into which some hydrogen diffusion takes place. This study clearly shows the power of high-resolution surface infrared spectroscopy. The sub-

tle differences observed in the vibrational spectrum of these two surfaces could only have been resolved using this particular technique. EELS cannot resolve the narrow peaks and Raman spectroscopy is not sensitive enough to probe submonolayers of atomic hydrogen. The ability to probe the polarization of vibrational modes has shown that the initial hydrogen adsorption is characterized by the formation of a monohydride.⁸ Only at higher coverage is the data consistent with dihydride formation.⁷ This behavior as a function of exposure was also observed in photon-stimulated desorption studies on the cleaved Si(111) surface.³⁹

ACKNOWLEDGMENTS

The authors would like to acknowledge discussions with L. C. Feldman, E. G. McRae, D. R. Hamann, and J. E. Rowe. Technical assistance was given by E. E. Chaban and M. E. Sims.

- ¹See, for example, E. G. McRae, *Surf. Sci.* **124**, 106 (1983), and references therein; G. Binnig, H. Rohrer, Ch. Gerber, and E. Weibel, *Phys. Rev. Lett.* **50**, 120 (1983); Y. J. Chabal, J. E. Rowe, and S. B. Christman, *Phys. Rev. B* **24**, 3303 (1981).
- ²D. M. Zehner, J. R. Noonan, H. L. Davis, and C. W. White, *J. Vac. Sci. Technol.* **18**, 852 (1981).
- ³D. M. Zehner, C. W. White, P. Heimann, B. Reihl, F. J. Himpsel, and D. E. Eastman, *Phys. Rev. B* **24**, 4875 (1981).
- ⁴R. M. Tromp, E. J. Van Loenen, M. Iwami, and F. W. Saris, *Solid State Commun.* **44**, 971 (1982).
- ⁵Y. J. Chabal, J. E. Rowe, and D. A. Zwemer, *Phys. Rev. Lett.* **46**, 600 (1981).
- ⁶T. Yokotsuka, S. Kono, S. Suzuki, and T. Sagawa, *Solid State Commun.* **39**, 1001 (1981).
- ⁷H. Wagner, R. Butz, U. Baches, and D. Bruchmann, *Solid State Commun.* **38**, 1155 (1981).
- ⁸Y. J. Chabal, *Phys. Rev. Lett.* **50**, 1850 (1983).
- ⁹Y. J. Chabal, E. E. Chaban, and S. B. Christman, *J. Electron Spectrosc. Related Phenom.* **29**, 35 (1983).
- ¹⁰E. E. Chaban and Y. J. Chabal, *Rev. Sci. Instrum.* **54**, 1031 (1983).
- ¹¹P. Hollins and J. Pritchard, *J. Vac. Sci. Technol.* **17**, 665 (1980).
- ¹²N. J. Harrick, *J. Opt. Soc. Am.* **55**, 851 (1965).
- ¹³R. J. Collins and H. Y. Fan, *Phys. Rev.* **93**, 674 (1954).
- ¹⁴Y. J. Chabal, S. B. Christman, E. E. Chaban, and M. T. Yin, *J. Vac. Sci. Technol. A* **1**, 1241 (1983); Y. J. Chabal and G. S. Higashi, *Bull. Am. Phys. Soc.* **28**, 860 (1983).
- ¹⁵K. J. Grant, P. Fisher, M. Kosaka, and A. M. Martin, *Aust. J. Phys.* **35**, 709 (1982), and references therein.
- ¹⁶R. J. Culbertson, L. C. Feldman, and P. J. Silverman, *J. Vac. Sci. Technol.* **20**, 868 (1982).
- ¹⁷T. Sakurai and H. D. Hagstrum, *Phys. Rev. B* **14**, 1593 (1976).
- ¹⁸L. C. Feldman, P. J. Silverman, and I. Stensgaard, *Nucl. Instrum. Methods* **168**, 598 (1980).
- ¹⁹D. H. Auston, J. A. Golovchenko, A. L. Simons, and C. M. Surko, *Appl. Phys. Lett.* **34**, 777 (1979).
- ²⁰E. G. McRae, *Surf. Sci.* **124**, 106 (1983).
- ²¹Y. J. Chabal, J. E. Rowe, and S. B. Christman, *J. Vac. Sci. Technol.* **20**, 763 (1982).
- ²²L. C. Snyder, Z. Wasserman, and J. W. Moskovitz, *J. Vac. Sci. Technol.* **16**, 1266 (1979).
- ²³J. Lander and J. Morrison, *J. Appl. Phys.* **34**, 1403 (1963); W. A. Harrison, *Surf. Sci.* **55**, 1 (1976).
- ²⁴M. J. Cardillo, *Phys. Rev. B* **23**, 4279 (1981).
- ²⁵E. G. McRae, *Phys. Rev. B* **28**, 2305 (1983).
- ²⁶F. J. Himpsel, *Phys. Rev. B* **27**, 7782 (1983).
- ²⁷L. C. Snyder, *Phys. Rev. B* (in press).
- ²⁸T. Sakurai and H. D. Hagstrum, *Phys. Rev. B* **12**, 5349 (1975).
- ²⁹H. Richter, H. J. Trodahl, and M. Cardona, *Bull. Am. Phys. Soc.* **28**, 532 (1983).
- ³⁰D. S. Girley and D. M. Haaland, *Appl. Phys. Lett.* **39**, 271 (1981).
- ³¹H. J. Stein and P. S. Peercy, *Appl. Phys. Lett.* **34**, 604 (1979).
- ³²M. H. Brodsky, M. Cardona, and J. J. Cuomo, *Phys. Rev.* **16**, 3556 (1977).
- ³³G. Lucovsky, R. J. Nemanich, and J. C. Knights, *Phys. Rev. B* **19**, 2064 (1979); W. B. Pollard and G. Lucovsky, *Phys. Rev. B* **26**, 3172 (1982); M. Cardona, *Phys. Status Solidi B* **117**, 437 (1983).
- ³⁴A less likely but intriguing explanation for this low-frequency band is the formation of three-center bonds on the Si(111) surface as described, for amorphous silicon, by L. C. Snyder, J. W. Moskovitz, and S. Topiol, *Phys. Rev. B* **26**, 6727 (1982). Such bonds would occur lower in frequency and contain a large component parallel to the surface.
- ³⁵Y. J. Chabal (unpublished).
- ³⁶L. Csepregi, E. F. Kennedy, J. W. Mayer, and T. W. Sigmon, *J. Appl. Phys.* **49**, 3906 (1978); J. Nishizawa, T. Terasaki, and M. Shimbo, *J. Cryst. Growth* **13-14**, 297 (1972).
- ³⁷P. A. Bennett, L. C. Feldman, Y. Kuk, E. G. McRae, and J. E. Rowe, *Phys. Rev. B* **28**, 3656 (1983).
- ³⁸P. M. Petroff and R. J. Wilson, *Phys. Rev. Lett.* **51**, 199 (1983); E. G. McRae (unpublished).
- ³⁹M. L. Knotek, G. M. Loubrid, R. H. Stulen, C. E. Parks, B. E. Koel, and Z. Hussain, *Phys. Rev. B* **26**, 2292 (1982).